Measurements, characteristics, and origin of new electromagnetic interference on magnetocardiographic measurements*

Gu Hong-Fang(谷红芳), Cai Wen-Yan(蔡文艳), Wei Yu-Ke(魏玉科), Liu Zheng-Hao(刘政豪), Wang Qian(王 倩), Wang Yue(王 越), Dai Yuan-Dong(戴远东), and Ma Ping(马 平)†

Applied Superconductivity Research Center of Peking University, Department of Physics, State Key Laboratory for Artificial Microstructure and Mesoscopic Physics, Peking University, Beijing 100871, *China*

(Received 28 November 2010; revised manuscript received 17 May 2011)

In order to eliminate the influence of the large-amplitude magnetic field noise that has complicated magnetocardiographic studies since October 2009, we have performed high-accuracy measurement of the environmental magnetic field noise in the vicinity of Beijing Subway Line 4 using a three-component height T_c radio frequency (rf) superconducting quantum interference device (SQUID). By analysing the spatial form and other characteristics of the time and the frequency domains and by calculating the circumferential magnetic field distribution based on a duel-end feeding system model, we reach the following conclusions: (i) the main source of magnetic field noise is the magnetic field generated by the subway trains, and (ii) the magnetic field interference results mainly from the imbalance between traction current and return rail current that is caused by the leakage current.

Keywords: electromagnetic interference, leakage current, subways, magnetocardiography

PACS: 07.55.Ge, 85.25.Dq, 52.70.Ds, 87.85.Ng **DOI:** 10.1088/1674-1056/21/4/040702

1. Introduction

Magnetocardiography (MCG) is a highly valuable and applicable method, but even now it has not been fully understood. It is difficult to measure desired magnetocardiography signals because they are several-orders lower (its maximum characteristic waveform is about 100 pT) than the geomagnetic pulsation (GP) and power-frequency magnetic fields (PFMF).[1,2] The frequency of MCG is extremely low and the energy of MCG is concentrated in a range below 30 Hz. It is well known that extremely-low-frequency weak magnetic fields are difficult to measure due to the following reasons: (i) quasi-static and extremely-low-frequency electromagnetic noises with high amplitudes and complex spectra exist everywhere on Earth, and most of these are caused by both human activity (electricity, telecommunications, etc.) and natural phenomena in the atmosphere, ionosphere, and even magnetosphere; (ii) all measuring instruments have intrinsic noises which increase as frequency decreases; (iii) effective shielding rooms are very expensive.

In order to make good use of the information contained in MCG, a high signal-to-noise (SN) ratio is required.[3,4] For this reason, MCG measurements necessarily involve not only high-resolution measuring instruments and suitable measuring environments, but also the employment of every possible method of eliminating the external magnetic field noises at frequencies that are relevant to MCG detection (such as methods derived from electronics, information theory and physics).

In the past, GP and PFMF were regarded as external noises that have the highest effect on the MCG SN ratio. Two ways of obtaining a high SN ratio are as follows: operate in a room that has high-performance shielding; and use a differential detection technique.

High SN ratio MCG, suitable for research and development, has been successfully obtained under

*Project supported by the State Key Development Program for Basic Research of China (Grant Nos. 2006CB601007 and 2011CBA00106), the National Natural Science Foundation of China (Grant No. 10674006), and the National High Technology Research and Development Program of China (Grant Nos. 2007AA03Z238 and 2007AA03Z213).

†Corresponding author. E-mail: maping@pku.edu.cn

© 2012 Chinese Physical Society and IOP Publishing Ltd

conurbation conditions by the Institute of Physics, Chinese Academy of Sciences, using a high T_c DC superconducting quantum interference device (SQUID) magnetometer[5] and by Peking University using high T_c rf SQUID.[6−8] Significant results were achieved in many areas of application, such as the MCG measurement of the human body, the MCG measurement based on the animal myocardial infarction model, the development of improved high T_c SQUID magnetometers, and other basic work for applications. All of these supplied useful data for research involving weak signal detection techniques and for biomagnetics and geophysics studies.[9,10]

At present, the urban infrastructure in China is in a period of rapid growth. The construction and operation of electrical facilities have caused serious disturbances for researchers trying detect and study weak signals. Since October 2009, Peking University's biomagnetism measurement system has been influenced by high-amplitude, low-frequency magnetic field noise with irregular occurrence times, as shown in Fig. 1. The main technical parameters of this system exhibit a significant downtrend, and many measurements cannot be conducted as usual during the day.

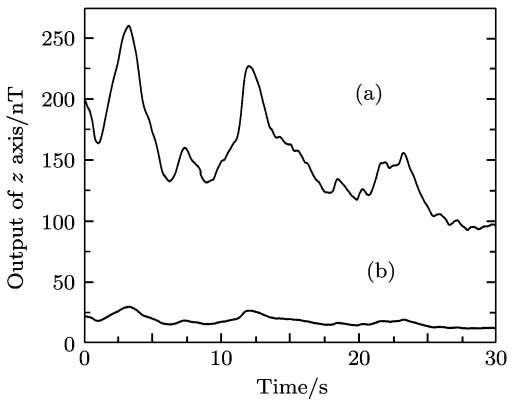


Fig. 1. Typical curves recorded by a three-component high T_c SQUID. Time of measurement: (a) 14:00 on 5/18/2010; (b) 14:10 on 6/10/2009 (before the subway began service for the day). Location: Peking University Physics Building, sampling rate: 1000 Hz, sampling time: 30 s.

In order to operate the original measurement system as usual, we continued to conduct an investigation on MCG in a new bio-magnetic measurement lab built in an unfavorable electromagnetic environment. We now need to find effective ways to weaken the influence of the interference. To achieve this goal, the origin, propagating path, and statistics properties of various magnetic field noises should be studied first.

In this paper, we carefully study low-frequency, large-amplitude environmental magnetic field noise using a high-resolution, wide-dynamic-range, three-component measuring system. This system consists of a simple shielding room, high T_c SQUID magnetometers, and a high-precision, real-time data acquisition system with a computer serving as the platform. Our analysis on time, frequency, and space domain data reveals that large-amplitude fluctuations are closely correlated with the running of subway trains. We thus confirm that the extremely low-frequency magnetic field noise comes from Subway Line 4. After analysis based on the electromagnetic induction law and the features of the subway's power supply and operation, we further conclude that the main sources are leakage current and the imbalance between traction current and return rail current.

2. Measurements

2.1. Method and apparatus

Measurements were performed at the biomagnetic laboratory in the Peking University Physics Building. The laboratory is located in the east of the East Gate of Peking University Station on the north–south Subway Line 4, with two main arterial roads nearby: the Chengfu Road 100 m away in the south, and the Baiyi Road 200 m away in the west.

During the operation of Subway Line 4, there appears an additional large-amplitude magnetic field noise. Preliminary observations show the new interference to be large in amplitude, low in frequency, and irregular in amplitude, time of occurrence, and period. In order to eliminate the influence of this noise and obtain high-quality MCG readings, we need to develop a proper data processing method. Technically, there are many possible choices. However, all of them need a full understanding of the characteristics of the source field and causes of the irregularity. Therefore, we conducted a long-term, high-accuracy observation project using the above-mentioned measuring system.

As stated above, the measuring system consists of a simple shielding room, a three-component high T_c rf SQUID magnetometer and a high-precision data acquisition system. Fabricated using three magnetometers that all have basically the same index, the three-component high T_c rf SQUID magnetometer has a high sensitivity, showing a white noise of about 300 fT/Hz$^{1/2}$ for each channel, and a voltage-magnetic

induction intensity conversion coefficient of about 30 mV/nT, a resolution better than 1 pT, a measurement range ±330 nT, and a linear dynamic range of over 120 dB. Within the simple shielding room, the measured magnetic field attenuation is 9 dB for DC magnetic field and 21 dB for PFMF. These parameters assure high-accuracy measurements of the magnetic field noise generated by the subway.

For measurements, we set the x axis pointing toward the west (the detection plane faced the Baiyi Road), the y axis toward the south (the detection plane faced the Chengfu Road), and the z axis downward (the detection plane faced the ground). The data acquisition system, which is constructed using the virtual instrument technique, was used exclusively for data acquisition, storage, and analysis. It consisted of three channels, each with a maximum sample ratio of 102.4 AKS/s, a resolution of 24-bit, and automatically adjustable (according to the output, i.e., the external magnetic field) input ranges of ±10 V, ±5 V, ±2 V, ±1 V, ±0.5 V, ±0.2 V or ±0.1 V. In this way, it was able not only to meet the high resolution requirements necessary for measuring weak signals but also to record the larger voltage output of the SQUID magnetometer.

2.2. Results

Variations with time in the environmental magnetic field were recorded using a three-component high T_c rf SQUID as shown in Fig. 2. The upper, the middle, and the lower curves denote the z, x, and y components, respectively.

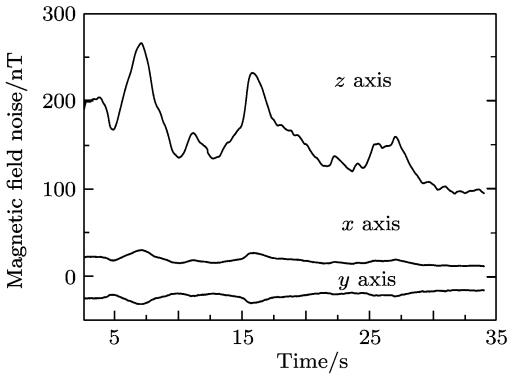


Fig. 2. Typical curves recorded by three-component high T_c SQUID. Time of measurement: 14:10 on 3/21/2010; location: Peking University Physics Building; sampling rate: 1000 Hz; Sampling time: 30 s.

In Fig. 2, obvious differences among the three components become observable. The x component and the y component have relatively small, low-frequency fluctuations. The x-axis detection plane faced the west and the y-axis detection plane faced the south. The reason why the x-component fluctuations are in the direction opposite to those y-component fluctuations is that the two SQUIDs have opposite polarities.

The z-axis output shows the largest low-frequency fluctuation. The z-component fluctuation range extends up to about 130 nT. The variation of z-axis output with time has the following characteristics: (i) low-frequency fluctuations with large large-amplitudes; (ii) unidirectional changes with time; (iii) periods of low-frequency fluctuation on the order of seconds; and (iv) fluctuations of unstable amplitude and period. Taking into account the idea that the magnetic field is caused by the current, these results show that the amplitude of the current changes irregularly with time, but its direction does not change in such a manner.

A 17-minute record of the z-axis output is shown in Fig. 3. The long-term record of the waveform reveals more clearly the high amplitude, the low frequency, the single direction, and the irregular amplitude, and the period of the magnetic field noise.

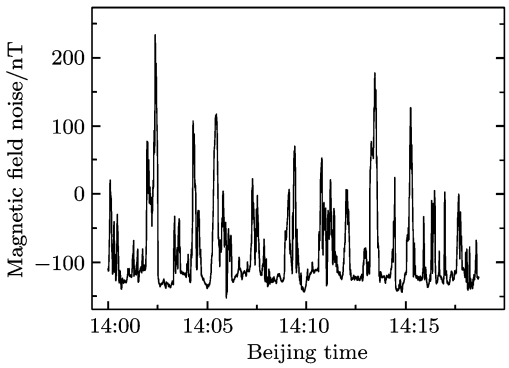


Fig. 3. Typical curve recorded by using the three-component high T_c SQUID. Time of measurement: 14:00 on 4/21/2010; location: Peking University Physics Building; sampling rate: 1000 Hz; sampling time: 17 min.

In order to fully understand the basic features of this magnetic field noise, we compare the power spectra of the various results in Fig. 3 using the fast Fourier transform (FFT) method. The corresponding noise spectra are given in Fig. 4.

We can see from Fig. 4 that the spectra of x, y, and z components recorded by the three-component SQUID system have similar forms. However there are significant differences in amplitude and the turning

point of the $1/f$ noise frequency among them. For example, the maximum amplitudes of white noises found in the x-, the y-, and the z-axes outputs are found to be $\leq$ 100 pT/Hz$^{1/2}$, $\sim$ 50 pT/Hz$^{1/2}$, and $\geq$ 100 pT/Hz$^{1/2}$, respectively, and the turning points to be 30 Hz, 10 Hz, and 80 Hz, respectively. The reason for these differences is that noises from the three directions came from different sources of magnetic interference.

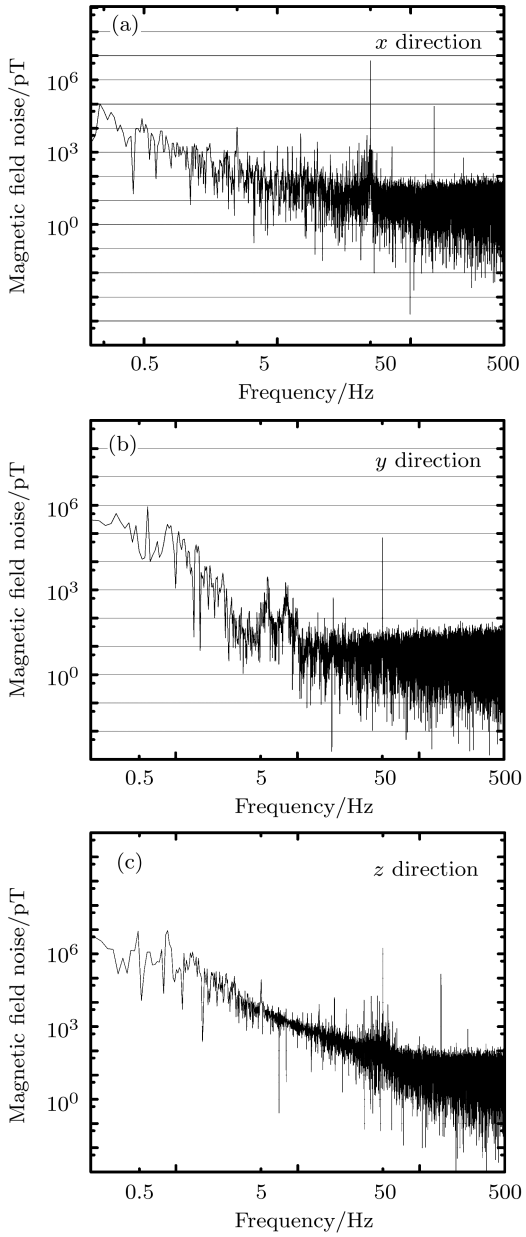


Fig. 4. Background magnetic field spectra obtained in (a) x direction, (b) y direction, and (c) z direction in the noisy environment with simple shielding.

The detection planes of the x-axis and the y-axis SQUID sensors were perpendicular to the ground (the detection plane of the y component faced the Chengfu Road and was perpendicular to Subway Line 4, the Baiyi Road, and the ground, while the detection plane of the x component faced the Baiyi Road and was perpendicular to Subway Line 4, the Chengfu Road, and the ground). The rolling stock of the Baiyi Road, Subway Line 4, and the traction current could give rise to low-frequency fluctuations of the largest amplitude. Relatively strong white noise came from the z-axis output.

To further identify the origins of the large low-frequency noise from the z component, we need to see waveforms (a) and (b) in Fig. 1, which represent the waveforms that were collected after and before the operation of Subway Line 4, respectively. We know that the traffic densities before and after the operation of Subway Line 4 do not change. With all the other conditions stay the same, we are able to eliminate the possibility that the large-amplitude fluctuations of the z component comes from heavy traffic. Thus, we conclude that the large fluctuations are probably generated by Subway Line 4.

The subway train is in service from 6:00 to 23:00. Taking into account the factors like the running time of the last train and train storage, we are able to determine that the time during which no train runs is from 24:00 to 5:00. If the large-amplitude, low-frequency fluctuations of the z-axis output are strongly correlated with running of subway trains, the fluctuations will disappear between 24:00 and 5:00. Therefore, we took measurements over a longer period of time, during the subway train running, stopping, and restarting times. Our measurement program lasted 8 h, from 23:00 to 7:00 the next morning, during which subway trains experienced light loads, overhauling, parking, restarting, heavy loads, and other phases of activity. Our observation data cover the entire situation of the magnetic field noise near the subway.

Figure 5 shows typical results of our observations. We can clearly see from Fig. 5 that before 23:50, the z-axis output has the same waveform and a similar amplitude fluctuation to those recorded during the day. At around 24:00, the amplitudes of the low-frequency fluctuations suddenly decrease and disappear and then remain unchanged until 5:00, at which time the outputs of the x, the y, and the z axes become nearly identical. However, at 5:40, the fluctuations reappear and exhibit similar characteristics to those before disappearing. This fits the subway timetable very well.

In addition, we can see in Fig. 5 that the maximum amplitude of the z-axis output is about 100 nT

before the subway train stops (at about 23:50), which is apparently lower than that recorded during the day (see Fig. 3). At around 7:00, larger-amplitude fluctuations of the z axis (up to 400 nT) appear. Comparing the fluctuations from around 7:00 with those from 14:00 (see Fig. 3), it can be seen that the fluctuations are larger during rush hours. Considering that the starting, acceleration, deceleration, and sliding of the train and even the number of passengers could change the current amplitude and its rate of change, it seems reasonable that there are differences in the amplitude and frequency of field noise at different times. In conclusion, inferred from the high correlation between magnetic field noise and the running of subway, this extremely-low-frequency interference is found to originate from Subway Line 4.

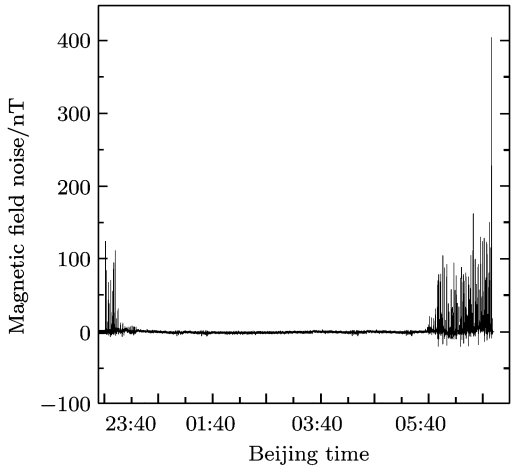


Fig. 5. Typical results recorded between 23:40 on 5/17/2010 and 6:40 on 5/18/2010.

3. Discussion

Theoretically, the time evolution and the spatial distribution of magnetic field noise can be deduced from the SQUID response output and its variation with time. However, the purpose of this project is to identify the origin of the magnetic field through qualitative analysis. For this reason, we start with the calculation of circumferential magnetic field distribution based on a duel-end feeding system and then compare the results with those of field experiments.

The subway trains in Beijing are power supplied with a 750-V DC source. The traction current is provided by the nearby third rail parallel to the trains, which is connected to a positive electrode of the substation (the source). The running rail is connected to a negative electrode of the substation, acting as the carrier of the return current. Figure 6(a) gives a schematic depiction of this power supply system.

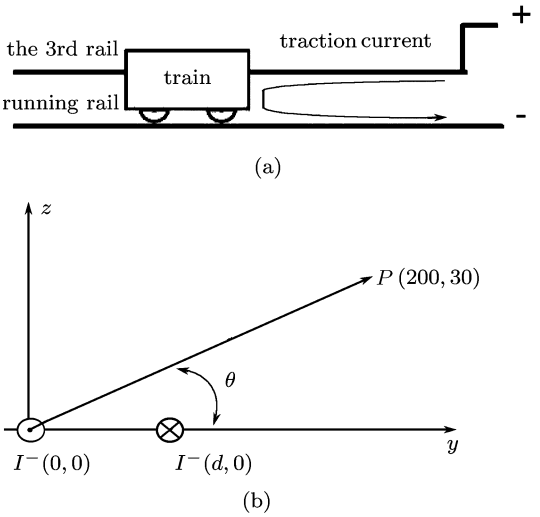


Fig. 6. (a) Schematic diagram and (b) theoretical model of the power transmission system.

Suppose that the rail tracks are fully insulated from the ground. The traction current completely returns to the negative electrode of the DC source. The magnetic field around the current system here resembles that of a pair of infinitely long, straight wires with equal but opposite electric currents (see Fig. 6(b)) if the relation $d \ll r \ll L$ is satisfied. Here, d is the distance between the wires, r is the distance between the measurement point and the geometric centre of the wires, and L is the length of the rail.

In Fig. 6(b), we consider the Earth as being isotropic and homogeneous with permeability equal to that of the free space μ_0. Because the measurement location was 200 m away from the subway, a distance that is far shorter than the length of the rail, the length of the power transmission lines can be regarded as being infinite. In our model, the line with the traction current (the third rail) and the line with the return current (the running rail) are located in the xy plane. We note that the third rail is located at the origin of the coordinate and the running rail is located at $y = d$. Traction current I^+ (0, 0) flows along the negative x axis (outward from the paper) with the return current I^- (d, 0) parallel to it in the opposite direction ($I^+ = I^-$). Considering that the attenuation for low-frequency magnetic noise is 9 dB (~ 8 times) in the shielding room, the horizontal and the vertical components of the magnetic field are as follows:

$$B_y = \frac{\mu_0 I d \sin 2\theta}{16\pi r^2}, \tag{1}$$

$$B_z = \frac{\mu_0 I d \cos 2\theta}{16\pi r^2}. \quad (2)$$

Taking the traction current as an independent variable, fluctuations in B_y and B_z varying with distance y, based on our yz-plane model, are shown in Fig. 7 (y denotes the y component of the measurement location P in the coordinate of Fig. 6(b)).

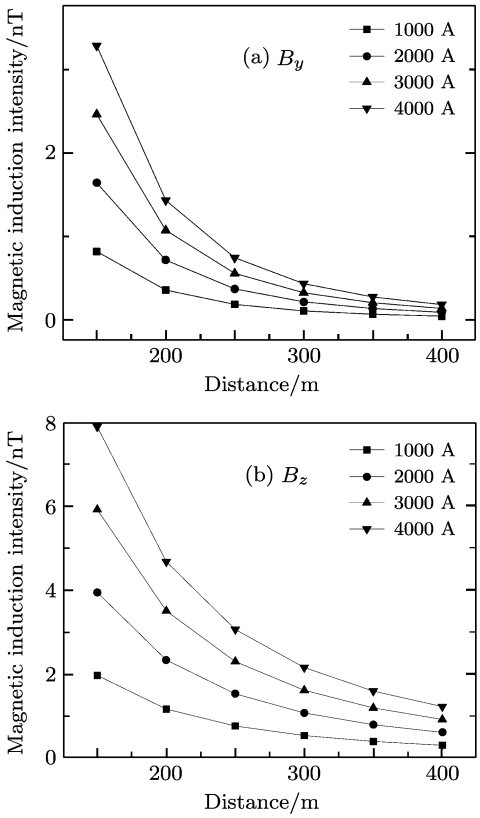


Fig. 7. Calculations of magnetic field based on an ideal model for $I = 1000$ A, 2000 A, 3000 A, and 4000 A.

In the ideal fully insulated system depicted above, the traction current I is 4000 A and the measurement location is 200 m away from the subway line. The amplitudes of fluctuation of the environmental magnetic field are 4.5 nT and 1.4 nT in the z and the y directions, respectively. In this ideal system, current can flow only within the circuit, so the magnetic field will decay rapidly with distance increasing. Comparing the amplitude of magnetic field noise shown in Fig. 3 with that shown in Fig. 7, this large-amplitude and low-frequency fluctuation of z component cannot appear in this ideal system.

In the real world, the full insulation between running rails and the ground is impossible. Due to the resistance between the ground and the running rails and to that of the running rails themselves, there is always a potential rise along the running rails, rail-to-earth voltage, and the leakage current (proportional to the return current) once the traction current of thousands of amperes goes through the power transmission system. Therefore, an actual power transmission system should consist of a third rail, a running rail, and the ground. Current from these three parts satisfies $I^+ = I^- + I_{\rm L}^-$, where I^+ is the traction current, I^- is the return rail current, and $I_{\rm L}^-$ is the leakage current.[11,12]

Suppose that the Earth is isotropic and homogeneous. There is a large conductivity interface for the current to leak into the ground, and the magnetic field generated by this leakage current is low in intensity and decays very quickly with distance increasing. Therefore, the traction current and the return current will be no longer be equal if leakage current exists.

It should be noted that there are many underground metallic elements in conurbations (pipelines, armored cables, earthing systems, reinforced concrete structures, etc). Because all of these have lower resistances than the Earth, such metallic structures can automatically play the role of carriers of the returning leakage current. Such processes are schematically depicted in Fig. 8.

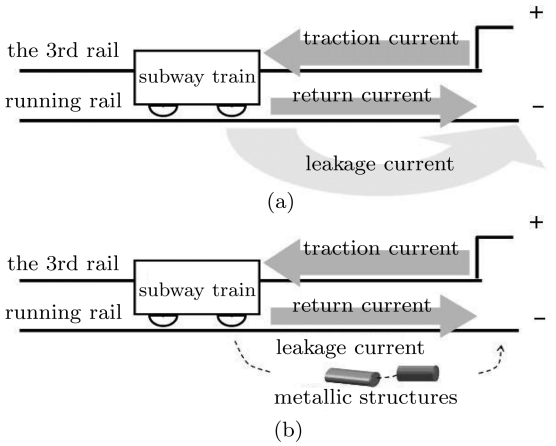


Fig. 8. Schematic diagrams of two situations in the real model.

Therefore, the environmental magnetic field noise from the subway can be related to the current imbalance between the power transmission lines and metallic structures along the path of the return current. Considering this, we add another current to Fig. 6 (see Fig. 9). The currents in Fig. 9 are related through $I^+ = I^- + I_{\rm L}^-$. Supposing $I^- = -0.9I^+$, this would indicate a 10% leakage of the traction current into the ground.

As shown in Fig. 8(a), the leakage current flows through isotropic and uniform soil which has a large resistance. In the simplest model, we can assume that the leakage current has the same intensity in every direction. In this case, the leakage current has a low density and a high decay rate. Thus we can ignore its contribution to the interference field. Based on the basic electromagnetic laws, the magnetic induction intensity at P (measurement location) can be expressed as follows:

$$B_z = \frac{\mu_0 I \cos\theta}{160\pi r} + \frac{9d\mu_0 I}{160\pi r^2}, \tag{3}$$

$$B_y = \frac{\mu_0 I \sin\theta}{160\pi r}, \tag{4}$$

where I is the traction current, r is the distance between P and the origin of coordinate O, and θ is the angle between the position vector $\boldsymbol{OP}$ and the y axis. The magnetic field is proportional to the inverse of the distance for the case of an infinitely long, straight electric current and proportional to the inverse of the distance squared for the case of two parallel, equal but opposite close currents. Therefore, we can regard the magnetic field distribution of two unbalanced currents as a superposition of the two situations depicted above. This means that the magnetic field of a power transmission system with leakage current will far exceed that of a system without leakage current. The calculated results based on the above equations are shown in Fig. 10 (in which y has the same definition as that in Fig. 7). From Fig. 10, we can see that the magnetic field in the real model is much larger than that in the ideal model. After the above qualitative analyses, we can reach the preliminary conclusion that the magnetic field interference relies heavily on the amplitude of the leakage current.

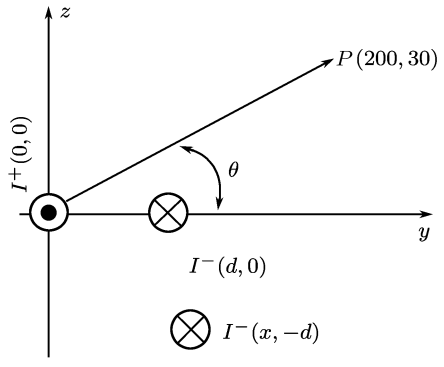


Fig. 9. Actual model of power transmission system.

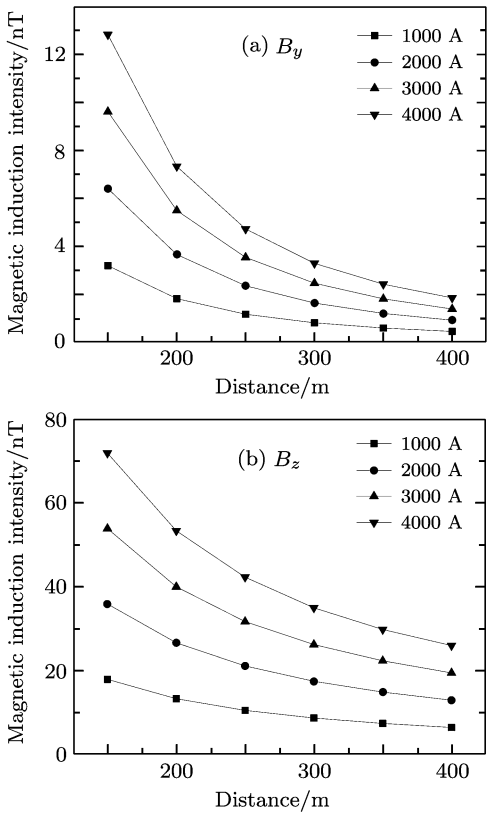


Fig. 10. Calculations of magnetic field based on the real model.

From the above discussion, we can conclude that the considerable environmental magnetic field fluctuations are caused by leakage current and the imbalance between the traction current and the return rail current.

We can analyse possible reasons for the irregularity in magnitude, time of occurrence, and period of the interference magnetic field fluctuations as follows. During our measurements, the resistance of the running rail was regarded as being constant and the subterranean electric conductivity as being uniform. Thus, the rail–earth voltage and the amplitude and the waveform of the leakage current were found to be correlated with the amplitude and the evolution process of the traction current when the trains started, accelerated, ran smoothly, and decelerated. As we have determined that the leakage current was the origin of the magnetic field noise, the instability was found to result from factors such as the train schedule, loads, and running conditions.

4. Conclusion

In this paper, we find that the magnetic field caused by the subway is able to influence magnetic

field measurements significantly. Even though its frequency is low, it is hard to eliminate its influence because of the irregularity in frequency, amplitude, and time of occurrence.

To start new magnetic field measurements or construct new MCG measurement systems in the areas around DC transmission lines, one must consider the range and the intensity of the magnetic field interference.

Considering that magnetic fields from long, straight currents decay rapidly with distance increasing, our high T_c rf SQUID magnetic measurement system, which has a shielding attenuation of about 9 dB for the case of extremely-low-frequency magnetic fields, fairly high magnetic field resolution, and a linear dynamic range of ± 370 nT, can be used for taking high-accuracy measurements of magnetic fields with large fluctuations, such as those near the subway.

In conclusion, the influence of the magnetic field from nearby DC power supply systems is inevitable. For weak magnetic field measurements in Peking University, the magnetic interference from the subway DC power supply system is attributed to the leakage-induced imbalance between the DC currents.

References

[1] Zhu X M, Ren Y F, Yu H W, Zhao S P, Chen G H, Zhang L H and Yang Q S 2006 *Chin. Phys.* **15** 100

[2] Nakaya Y and Mori H 1992 *Clin. Phys. Physio. Meas.* **13** 191

[3] Cohen D, Edelsack E A and Zimmerman J E 1970 *Appl. Phys. Lett.* **16** 278

[4] Wang Q, Ma P, Lu H, Tang X Z, Hua N and Tang F K 2009 *Chin. Phys.* B **18** 5566

[5] Wang H W, Kong X Y, Ren Y F, Yu H W, Ding H S, Zhao S P, Chen G H, Zhou Y L, Zhang L H, He Y S and Yang Q S 2004 *Chin. Phys.* **13** 19

[6] Drung D 1955 *IEEE Trans. Appl. Supercond.* **5** 2112

[7] Wakai R T, Wang M and Martin C B 1994 *Am. J. Obstet. Gynecol.* **170** 770

[8] Jeng J T, Horng H E and Yang H C 2002 *Physica* C **368** 105

[9] Li Z, Chen G H, Zhang L H, Yang Q S and Feng J 2006 *Chin. Phys.* **15** 310

[10] Zhang M J, Lang P L, Peng Z H, Chen Y F, Chen K and Zheng D N 2006 *Chin. Phys.* **15** 1903

[11] Lowes F J 1987 *Physics in Technology* **18** 209

[12] Lee C H 2005 *IEEE Transactions on Power Delivery* **20** 1379